Development 134, 3383-3392 (2007) doi:10.1242/dev.005181

GLH-1, the *C. elegans* P granule protein, is controlled by the JNK KGB-1 and by the COP9 subunit CSN-5

April M. Orsborn[1,*], Wensheng Li[1,†], Tamara J. McEwen[1], Tomoaki Mizuno[2], Evgeny Kuzmin[1], Kunihiro Matsumoto[2] and Karen L. Bennett[1,‡]

The GLHs (germline RNA helicases) are constitutive components of the germline-specific P granules in the nematode *Caenorhabditis elegans* and are essential for fertility, yet how GLH proteins are regulated remains unknown. KGB-1 and CSN-5 are both GLH binding partners, previously identified by two-hybrid interactions. KGB-1 is a MAP kinase in the Jun N-terminal kinase (JNK) subfamily, whereas CSN-5 is a subunit of the COP9 signalosome. Intriguingly, although loss of either KGB-1 or CSN-5 results in sterility, their phenotypes are strikingly different. Whereas *csn-5* RNA interference (RNAi) results in under-proliferated germlines, similar to *glh-1/glh-4(RNAi)*, the *kgb-1(um3)* loss-of-function mutant exhibits germline over-proliferation. When *kgb-1(um3)* mutants are compared with wild-type *C. elegans*, GLH-1 protein levels are as much as 6-fold elevated and the organization of GLH-1 in P granules is grossly disrupted. A series of additional in vivo and in vitro tests indicates that KGB-1 and CSN-5 regulate GLH-1 levels, with GLH-1 targeted for proteosomal degradation by KGB-1 and stabilized by CSN-5. We propose the 'good cop: bad cop' team of CSN-5 and KGB-1 imposes a balance on GLH-1 levels, resulting in germline homeostasis. In addition, both KGB-1 and CSN-5 bind Vasa, a *Drosophila* germ granule component; therefore, similar regulatory mechanisms might be conserved from worms to flies.

KEY WORDS: Germline, MAPK docking site, Signalosome, Degradation, Phosphodegron, Vasa, Homeostasis

INTRODUCTION

Germ granules, key elements in germline development, are found in most animals. These structures are classic germline determinants. In *Caenorhabditis elegans*, germ granules are known as P granules, non-membranous aggregates of protein and RNA found exclusively in the germline (Strome and Wood, 1982; Strome and Wood, 1983). The four germline RNA helicases (GLHs) are constitutive P granule components (Gruidl et al., 1996; Kuznicki et al., 2000; Roussell and Bennett, 1993). GLH proteins are similar to *Drosophila* Vasa, a component of the polar (germ) granules in flies (Hay et al., 1988a; Hay et al., 1988b; Lasko and Ashburner, 1988). Like Vasa, GLHs are putative DEAD-box RNA helicases, but GLHs differ by the presence of multiple CCHC zinc fingers and all but GLH-3 have N-terminal, glycine-rich repeats. The loss of *glh-1* by RNA interference (RNAi) causes sterility in *C. elegans* when worms are raised at the restrictive temperature of 26°C, whereas combinatorial RNAi of *glh-1* and *glh-4* causes sterility even at the normally permissive temperature of 20°C (whereas *glh-2* and *glh*-3 have no apparent effects when knocked down by RNAi, nor as deletion mutants) (Kuznicki et al., 2000) (K.L.B., unpublished). *glh-1/glh-4(RNAi)* results in nematodes with under-proliferated germlines that contain about one-third as many germ cells as wild type, with no functional sperm or oocytes produced (Kuznicki et al., 2000). A yeast two-hybrid screen identified several GLH-interacting proteins (Smith et al., 2002). In this study, we report that two GLH binding partners, KGB-1 (kinase that GLHs bind) and CSN-5 (COP9 signalosome subunit 5), associate with each other and are likely to regulate GLH-1 levels.

The GLH binding partner KGB-1 is a MAP kinase of 390 amino acids and a member of the Jun N-terminal kinase (JNK) subfamily (Ip and Davis, 1998; Robinson and Cobb, 1997). KGB-1 has a novel, yet functional, activation site that consists of SDY rather than TPY (Mizuno et al., 2004); this activation site is only found in two other MAP kinases, the *C. briggsae* KGB-1 homolog that is 88% identical to KGB-1, and the *C. elegans* KGB-2 protein that matches KGB-1 with 86% identity, but has no discernible phenotype when deleted (Mizuno et al., 2004) (K.L.B., unpublished). Aside from this activation site, KGB-1 is very similar to the *Drosophila* MAP kinase Basket (BSK) (53% identical and 67% similar) and the human MAPK10 (52% identical and 68% similar) (www.wormbase.org). The mutant *kgb-1(um3)*, which is missing more than 1.2 kb that includes most of the kinase domain, exhibits a temperature-sensitive sterile phenotype. At 26°C, *kgb-1* worms have larger than normal gonads containing many endomitotically replicating oocytes (EMO) (Smith et al., 2002). As the *kgb-1(um3)* mutant was used almost exclusively, when *kgb-1* is used in the text, it refers to the *kgb-1(um3)* allele.

The JNKs are involved in signaling cascades that regulate development in many organisms, including *Drosophila*, in which JNK mutants have disrupted embryonic dorsal closure and defects in apoptosis and wound healing (Adachi-Yamada et al., 1999; Bosch et al., 2005; Igaki et al., 2002; Jacinto et al., 2002; Mattila et al., 2005). In *C. elegans*, the JNK family members JNK-1 and KGB-1 are known to respond to the stress of bacterial infections or exposure to heavy metals (Huffman et al., 2004; Koga et al., 2000; Mizuno et al., 2004).

CSN-5 is the most highly conserved subunit of the COP9 signalosome, a complex in plants and animals that regulates protein stability through SCF ubiquitin ligases (for reviews, see Chamovitz and Glickman, 2002; Cope and Deshaies, 2003). CSN-5 can stabilize some targets and promote the degradation of others,

[1]Molecular Microbiology and Immunology Department, University of Missouri, Columbia, MO 65212, USA. [2]Molecular Biology Department, Nagoya University, Chikusa-ku, Nagoya 464-8602, Japan.

*Present address: Molecular Biology Department, UC Berkeley, Berkeley, CA 94720-3200, USA
†Present address: Mayo Clinic Jacksonville, Jacksonville, FL 32224, USA
‡Author for correspondence (e-mail: bennettk@missouri.edu)

Accepted 2 June 2007

functioning alone or in the CSN complex. Proteins including p53 (the well-known tumor suppressor), rat lutropin/choriogonadotropin, p27Kip1 (also known as Cdkn1b) and the *Arabidopsis* auxin responsive proteins (IAAs) are degraded by CSN-mediated ubiquitination (Bech-Otschir et al., 2001; Li et al., 2000; Schwechheimer et al., 2001). By contrast, the transcriptional regulators c-Jun, Id1 and Id3 are protected from degradation by their interactions with CSN. In *C. elegans*, CSN-5 orchestrates the degradation of MEI-1, a protein that functions after fertilization in the switch from meiosis to mitosis (Pintard et al., 2003). CSN-5 also binds the GLHs, with loss of *csn-5* mirroring *glh-1/glh-4(RNAi)* (Kuznicki et al., 2000; Smith et al., 2002); these results are consistent with CSN-5 stabilizing GLH proteins, as indicated for GLH-1 by this work.

In *C. elegans*, regulation of protein degradation has been elegantly examined in relation to embryonic patterning and the transition from oocyte to embryo (DeRenzo et al., 2003; Reese et al., 2000; Nishi and Lin, 2005; Pellettieri et al., 2003; Shirayama et al., 2006; Stitzel et al., 2006). As GLH-1, GLH-4, KGB-1 and CSN-5 are each important for adult fertility, these studies focused on the adult germline. The *C. elegans* germline develops from the single germline precursor P4 cell that divides once in the embryo to produce the germline progenitor cells Z2 and Z3, which arrest until during the second larval stage (L2). The rate of germline mitosis increases in the third larval stage (L3), and spermatogenesis initiates and completes in the fourth larval stage (L4), with sperm then stored in the spermatheca, awaiting the production of oocytes. After the L4/adult molt, the syncytial germ cells switch to oogenesis. With the completion of the pachytene stage of meiosis, oocytes cellularize and mature in a single-file, assembly-line fashion. After maturation, individual oocytes pass through the spermatheca and are fertilized, with the resulting embryos retained by the mother while they undergo several cell divisions. Thus, the bi-lobed gonad of the *C. elegans* adult contains a continuum – from germ cell nuclei in mitosis and meiosis to mature sperm, oocytes and developing embryos (see Fig. 2A). *C. elegans* become young adults within 12 hours of the L4 stage and produce most of their ~300 progeny in the next 3 days, with all aspects of development occurring more rapidly at 26°C than at 20°C (Epstein and Shakes, 1995).

MATERIALS AND METHODS

Western blot analysis

To compare GLH-1 protein levels, equal numbers of animals were picked at the L4 stage and maintained at 20°C or 26°C for the indicated times. Lysates were analyzed using SDS-PAGE and western blotting. Rabbit antibodies against GLH-1 and GLH-4 were used at 1:1000, whereas mouse anti-α-tubulin (Santa Cruz) or anti-β-tubulin antibodies (Sigma) were diluted 1:1000 and 1:10,000, respectively. Goat anti-rabbit or goat anti-mouse secondary antibodies conjugated to horseradish peroxidase (ICN) were used at 1:10,000. The C-terminal rabbit C2-2 anti-KGB-1 antibody (Mizuno et al., 2004) was used at 1:500. Western blots were developed using Supersignal West Pico or Dura chemiluminescence (Pierce) and exposed to film or phosphorimaging plates. Films were processed using Adobe Photoshop. A BioRad FX phosphorimager and Quantity One software were used for quantification.

Northern blot analysis

Total RNA was isolated from adult N2 and *kgb-1* animals grown at either 20°C or 26°C from the L1 stage. RNA was extracted using Trizol (Invitrogen) as described (Reinke et al., 2000). RNA samples were run on MOPS-acrylamide gels and transferred to nylon membranes. Probes specific to *glh-1*, *glh-4*, *kgb-1* or to *eIF-4A* (Roussell and Bennett, 1993) were generated using the Prime-It II Kit (Stratagene).

Immunocytochemistry

N2 and *kgb-1(um3)* or *kgb-1(km21)* (Mizuno et al., 2004) animals were grown at 20°C or 26°C; L4 worms were isolated and adults analyzed as described (Kuznicki et al., 2000). For GLH-1 and KGB-1 localizations, gonads were fixed for 1 hour in 3% formaldehyde/0.1 M K_2HPO_4 pH 7.2 at room temperature, followed by 5 minutes in methanol at –20°C (Jones et al., 1996). For PGL-1, slides were fixed in methanol, then in acetone, both for 15 minutes at –20°C (Kawasaki et al., 1998). Anti-PGL-1 antibody was used at 1:3000, with anti-GLH-1 at 1:500-1:2000. The anti-KGB-1 antibodies used for immunocytochemistry were generated in mice with the N-terminal KGB-1-specific peptide, MEVDLPVHNEYDASRFHQVT, conjugated to KLH (keyhole limpet hemocyanin). Combined sera from two positive mice were affinity purified with high salt (5 M KI) (Olmstead, 1986); preimmune and hyperimmune sera were diluted 1:2. Fluorescent secondary antibodies (Alexa Fluor, Molecular Probes) were diluted 1:3000. Images were recorded with a Spot CCD camera on a Zeiss Axioplan microscope. When comparing images, the same exposure was used.

GST pull-down experiments

GST pull-downs were performed with baculovirus-expressed proteins in HighFive insect cells (Invitrogen) as described (Smith et al., 2002). Proteins were tagged with GST or 6-His and cloned into pFastBac (Invitrogen). Constructs were sequenced to verify that intact proteins would be produced. For protein homogenates, N2 and *kgb-1(um3)* worms were grown in liquid culture (Epstein and Shakes, 1995) to the adult stage, washed, frozen in liquid nitrogen, thawed in PBS and then lysed by three passages through a French pressure-cell under 900 psi. Lysates were centrifuged for 10 minutes at 10,000 ***g***, removing insoluble materials. For experiments using expressed proteins combined with *C. elegans* lysates, 1 mL insect-cell lysate mixed with 3 mL worm lysate was incubated at 4°C for 2 hours with 500 μL 1:1 (v/v) Glutathione-Uniflow Resin:PBS (BD Biosciences Clonetech). Beads were washed four times in 1 mL PBS containing 1% Triton X-100 and proteins eluted and analyzed as described above.

Site-directed mutagenesis

Primers deleting the GLH-1 D site, or changing the lysine at 581 to asparagine, and then changing the leucines at positions 588 or 589 to tryptophan were generated using directions from the Quick Change II Site-Directed Mutagenesis manual (Stratagene). PCR for site-directed mutagenesis, following the manufacturer's protocol (Stratagene), was performed on GLH-1 in the pFastBac plasmid, and clones were sequenced to verify the mutations.

Kinase assays

Immunoprecipitations and kinase assays were performed as previously described, using GST-tagged GLH-1 (Mizuno et al., 2004).

Proteasome and JNK inhibitor experiments

HighFive cells (Invitrogen) were grown and treated as in GST pull-down analysis above, except that cells were grown for 18 hours at 26°C after infection and then treated (or not) with 1 μM MG132 (Calbiochem) for 5 hours, before harvesting. Protein homogenates were analyzed by western blot to examine GLH-1-6-His levels using anti-His antibody (Santa Cruz Biotech) diluted 1:2000. For the in vivo tests, young N2 adults were grown in standard liquid culture at 20°C with either 1 μM MG132, 50 μM JNK inhibitor (SP600125, CalBiochem) or no inhibitor added. Inhibitor was added for varying amounts of time, but all worms were grown for a total of 6 hours and analyzed for GLH-1 by western blot (50 worms/lane), using α-tubulin (Sigma) at 1:5000 as the loading control. After Dura chemiluminescence (Pierce), quantification employed Multigauge software (Fuji)

RNA interference

RNAi was performed for *glh-1* and *csn-5* as described (Kuznicki et al., 2000; Smith et al., 2002). For *actin*, a 446 nt dsRNA that has one mismatch/primer for each of the five *C. elegans actin* genes (*act-1-5*) was produced using primers from Gao et al. (Gao et al., 2006). For *pan-1* (cosmid M88.6), primers 5′-GTAATACGACTCACTATAGGGCGCGAAGCTTAC-3′ and

5′-GTAATACGACTCACTATAGGGCCTGGAATCGTACAG-3′ were used that contain T7 RNA polymerase sites and produce a 1742 nt full-length *pan-1* product (G. Gao and K.L.B., unpublished). All dsRNAs were injected at ~1 mg/mL. Fertile *kgb-1; csn-5(RNAi)* F_1 animals, raised at 20°C, were only counted when the mother also produced sterile F_1 siblings.

RESULTS

kgb-1(um3) mutants have increased GLH-1 levels

To examine in vivo interactions between KGB-1, CSN-5 and the GLHs, we began with western blot analyses of GLH-1 and GLH-4 proteins, using wild-type (N2) and *kgb-1* worms. As there are no migration differences either in GLH-1 or GLH-4 when N2 and *kgb-1* mutants are compared (Fig. 1A,C), if KGB-1 phosphorylates the GLHs, these proteins are either rapidly eliminated or this modification does not result in a detectable alteration in migration. However, western blots of equal numbers of *kgb-1* and N2 adults synchronously grown beyond the L4 stage revealed higher GLH-1 levels in the *kgb-1* mutants than in N2 worms, both at 20°C and 26°C. These differences were statistically significant for GLH-1 at all stages except for the youngest adults grown at 20°C, whereas GLH-4 showed little difference between the strains (Fig. 1A-D). Comparing N2 and *kgb-1* adults revealed that GLH-1 levels were as much as 6-fold higher in *kgb-1* mutants than in N2s.

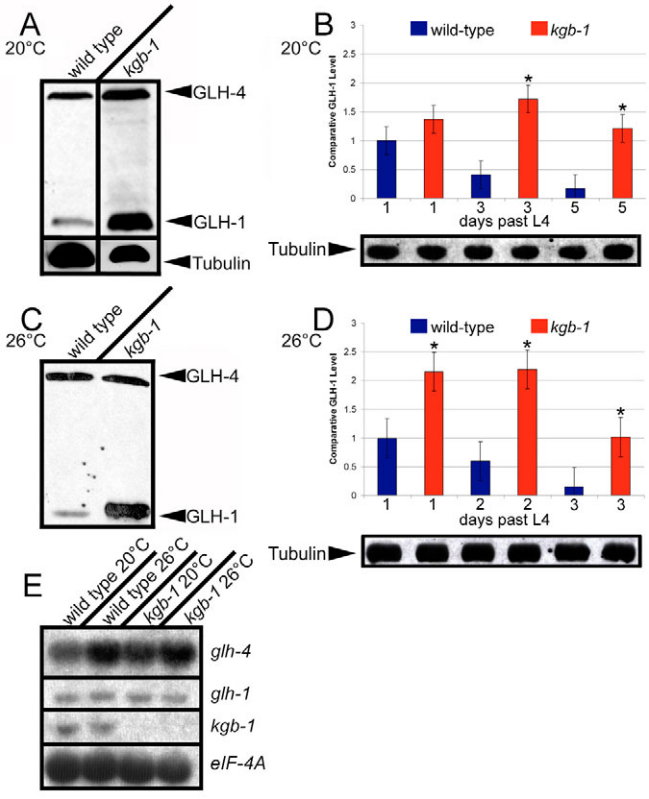

Fig. 1. GLH-1 levels are increased in *C. elegans kgb-1* mutants. (**A**) N2 (wild-type) and *kgb-1* worms grown at 20°C for 5 days beyond (d>) the L4 stage were analyzed by western blot (1000 worms in the wild-type lane and 800 worms in the *kgb-1* lane), examining GLH-1 and GLH-4; β-tubulin was a loading control. (**B**) Relative levels of GLH-1 in *kgb-1* and N2 worms were compared for 1, 3 and 5 d>L4 at 20°C, with GLH-1 levels for N2 worms at 1d>L4 set to 1 and other levels determined relative to this. Values are the average of three experiments, with the standard error shown. *, differences in GLH-1 between *kgb-1* and N2 are statistically significant ($P<0.05$). Beneath, a representative blot with a β-tubulin loading control is shown. For B-D, 600 worms were loaded per lane. (**C**) N2 and *kgb-1* worms grown at 26°C for 3.5d>L4 were analyzed by western blot to examine GLH-1 and GLH-4 levels. (**D**) GLH-1 levels were quantified for N2 worms and *kgb-1* mutants grown at 26°C for 1, 2 and 3d>L4. *, GLH-1 differs significantly between N2 and *kgb-1* animals ($P<0.05$). β-tubulin was the loading control. (**E**) Northern blot analysis of RNA from N2 and *kgb-1* adults grown at 20°C or 26°C shows relative abundance of *glh-4*, *glh-1* and *kgb-1* transcripts, with an *eIF-4A* loading control. The *kgb-1* probe did not include the 5′ end of the gene, for which RT-PCR detects a small product in *kgb-1(um3)* RNA (not shown).

To investigate whether the increase in GLH levels observed in *kgb-1* worms was due to an increase in *glh* transcript accumulation, total RNA from N2 and *kgb-1* adults was analyzed. Little or no differences in *glh-4*, *glh-1* or *kgb-1* transcript levels were found when N2 and *kgb-1* RNAs were compared, with the exception that no *kgb-1* transcript was detected in the *kgb-1* mutant (Fig. 1E). Therefore, the increase in GLH-1 observed in *kgb-1* worms appears to be due to regulation by the KGB-1 kinase of GLH-1 protein, and not to an effect of KGB-1 on the production or stability of *glh-1* or *glh-4* mRNA.

kgb-1 mutants have abnormal P granules and extra germ cells

Results from immunocytochemistry of N2 and *kgb-1* mutants support the increased GLH-1 levels seen by western analysis. When wild-type and *kgb-1* worms of the same age were compared, fluorescence corresponding to GLH-1 in the adult germline was much brighter in *kgb-1* worms than in their wild-type counterparts (Fig. 2, E versus D). In wild-type worms, GLH-1 was present in punctate P granules, with each germ cell nucleus surrounded by multiple P granule clusters (Fig. 2D,F). By contrast, *kgb-1* mutants were found to have greatly increased staining for GLH-1, and instead of being localized in discrete P granules, GLH-1 protein was disorganized, completely surrounding the germ cell nuclei (Fig. 2E,G). Also, *kgb-1* gonads were somewhat bigger than N2 gonads (Fig. 2, C versus B) and sterile *kgb-1* hermaphrodites had 22% more germ cell nuclei than wild type, with an average of 510 ($n=6$) nuclei per *kgb-1* gonad arm, compared with 419 nuclei per N2 gonad arm ($n=10$), with both strains grown under the same conditions. This increase is statistically significant ($P<0.04$). Although extra germ cells could result from a back-up of healthy oocytes due to defective sperm, this is unlikely to be the case in *kgb-1* worms because mating with N2 males does not rescue the *kgb-1* sterility, as it does for the *fem-1(hc17)* strain (Nelson et al., 1978; Smith et al., 2002). In addition, both the masculinized *fem-3(q24)(gf)* and the feminized *fem-1(hc17)(lf)* strains have higher *glh-1* mRNA levels than wild-type worms (Roussell and Bennett, 1993); therefore, it is unlikely that the *kgb-1* defect is similar to the defects in these other strains. Thus, the *kgb-1(um3)* mutation, although it may affect sperm, is most apparent in germline proliferation and oogenesis.

PGL-1, also a constitutive component of P granules and one that depends upon GLH-1 for its localization (Kawasaki et al., 1998), was also elevated in *kgb-1* animals (see Fig. S1, C versus A, in the supplementary material).

KGB-1 is uniformly cytoplasmic in the distal germline, becoming particulate in oocytes

To determine where KGB-1 localizes in the germline, we generated anti-KGB-1 polyclonal antibodies with an N-terminal KGB-1-specific peptide (Fig. 3A-E); these mouse antibodies were used in conjunction with rabbit anti-GLH-1. As shown previously, in the distal gonad GLH-1 surrounds each germ cell nucleus; however, when oocytes cellularize and enter diakinesis, the GLH proteins and

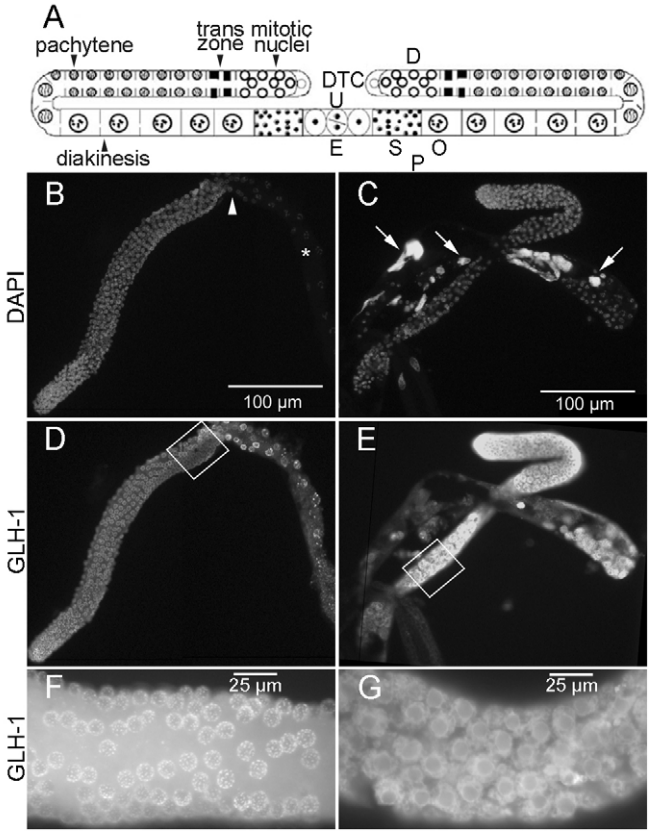

Fig. 2. *kgb-1* mutants have more GLH-1 with grossly expanded P granules. (**A**) Schematic of the adult *C. elegans* germline adapted from Navarro et al. (see Navarro et al., 2001; Smith et al., 2002). Both gonad arms are shown, containing mitotic nuclei, the transition zone from mitosis to meiosis, the pachytene region and the diakinetic region where oocytes cellularize. DTC, distal tip cell; D, distal gonad; E, embryo; U, uterus; S, sperm; P, proximal gonad; O, mature oocyte. (**B**) One arm of a splayed gonad from an N2 worm grown at 26°C for 2d>L4 (DAPI-stained). Germ cell nuclei in pachytene (arrowhead) and diakinesis (asterisk) are indicated. (**C**) A *kgb-1* mutant treated as in B shows one gonad arm wrapped on itself, with the distal end at the top and the proximal end to the right (DAPI). Examples of EMO (endomitocially-replicating) nuclei are indicated with arrows. (**D**) Gonad in B with anti-GLH-1 antibody. (**E**) Gonad in C with anti-GLH-1 antibody. (**F**) Magnified view (1000×) of the pachytene region of the N2 gonad (the boxed region from D). (**G**) Magnified view (1000×) of the *kgb-1* gonad (the boxed region from E).

the P granules dissociate from their peri-nuclear location and disperse throughout the cytoplasm (Fig. 3B) (Kuznicki et al., 2000; McCarter et al., 1999; Pitt et al., 2000; Strome and Wood, 1982). We found that KGB-1 is uniformly cytoplasmic in the distal gonad, overlapping in location with GLH-1 (Fig. 3C-E) and, like GLH-1, disperses into particles when oocytes cellularize (Fig. 3C and see Fig. S2 in the supplementary material); however, the GLH-1 and KGB-1 puncta were often distinct from one another (Fig. 3D,E). Therefore, KGB-1 and GLH-1 could interact during proliferation and meiosis and dissociate after GLH-1 leaves its peri-nuclear location. Interestingly, in maturing oocytes, the GLH binding partner CSN-5 remains uniformly cytoplasmic and is also concentrated in a subnuclear location, perhaps no longer bound to GLH-1 (Fig. 6C) (Smith et al., 2002). In contrast to KGB-1 particles, which were found in multiple oocytes (Fig. 3C and see Fig. S2 in the supplementary material), the activated form of the well-studied MAP kinase, MPK-1, is most visible in the most proximal oocyte. MPK-1, like KGB-1, is required for progression out of pachytene and additionally controls meiotic oocyte maturation (Church et al., 1995; Miller et al., 2001; Page et al., 2001; Smith et al., 2002). However, the commercial phospho-specific MPK antibodies (Sigma) only detect active MPK, whereas the anti-KGB-1 antibodies are likely to detect all forms of KGB-1; therefore, it remains to be determined whether the activated forms of these two MAPKs have similar localization patterns. In summary, KGB-1 and GLH-1 overlap in the cytoplasm of the distal germline and resolve into discrete particles in developing oocytes. This pattern is likely to reflect a very dynamic relationship between GLH-1 and KGB-1. Perhaps phosphorylation by KGB-1 signals GLH-1 to leave the nuclear membrane and be targeted for degradation.

KGB-1 and GLH-1 interact in vivo

As a biochemical test of the in vivo KGB-1–GLH-1 interaction, we used GST-tagged GLH-1 protein to pull KGB-1 out of *C. elegans* protein lysates. We found that GLH-1-GST is able to precipitate KGB-1 from wild-type nematode lysate, whereas GST alone does not (Fig. 4A, lane 5 versus 4). As a negative control, incubation of GLH-1-GST with *kgb-1* lysate did not result in detectable precipitation of KGB-1 (Fig. 4C, lane 6), although the *kgb-l* lysate did contain endogenous GLH-1 (Fig. 4A, lane 2) and did not detect KGB-1 (Fig. 4C, lane 1). Thus, in *C. elegans* lysates, GLH-1 interacts with native KGB-1.

Taken together, our various in vivo studies suggest an essential interaction between KGB-1 and GLH-1. When the kinase function of KGB-1 is missing, GLH-1 protein levels increase, P granule structure appears disrupted, oogenesis is defective and the numbers of germ cell nuclei increase. Along with these relationships revealed by the *kgb-1(um3)* mutant, in wild-type worms KGB-1 and GLH-1 resolve into discrete sets of particles as P granules leave the nuclear membrane during oogenesis. Therefore, KGB-1, a GLH-1 binding partner, controls GLH-1 protein levels and coordinates the organization of GLH-1 in P granules.

Biochemical interactions between KGB-1 and GLH-1

In considering how KGB-1 might regulate GLH-1, we compared the predicted protein sequences of GLH-1 and GLH-4 and found that GLH-1 contains a consensus MAPK D (docking) site. This site is not completely conserved in GLH-4 (one mismatch in each of two possible motifs, Table 1). MAP kinases bind their target substrates via D sites, characterized by an LxL motif 1-5 amino acids downstream from several basic amino acids (Jacobs et al., 1999) (reviewed by Sharrocks et al., 2000). GLH-1 also contains a consensus phosphodegron, an additional motif used by some MAP kinases to phosphorylate their substrates and target them for degradation. Again, neither of two potential GLH-4 phosphodegron motifs completely corresponds to consensus (Table 1). Phosphorylation at phosphodegron sites is responsible for the timely and rapid degradation of the cell cycle proteins mammalian cyclin E and the yeast CDK (cyclin-dependent kinase) inhibitor Sic1 (Orlicky et al., 2003; Ye et al., 2004). D sites and phosphodegrons allow for coordinated protein recognition and degradation in response to a wide range of stimuli and stresses. Therefore, these motifs could be important if GLH-1 levels are controlled by KGB-1 phosphorylation that leads to degradation.

Previous GST pull-down assays had established that KGB-1 and GLH-1 interact when co-expressed in baculovirus (Smith et al., 2002). We expanded upon these pull-downs by testing several

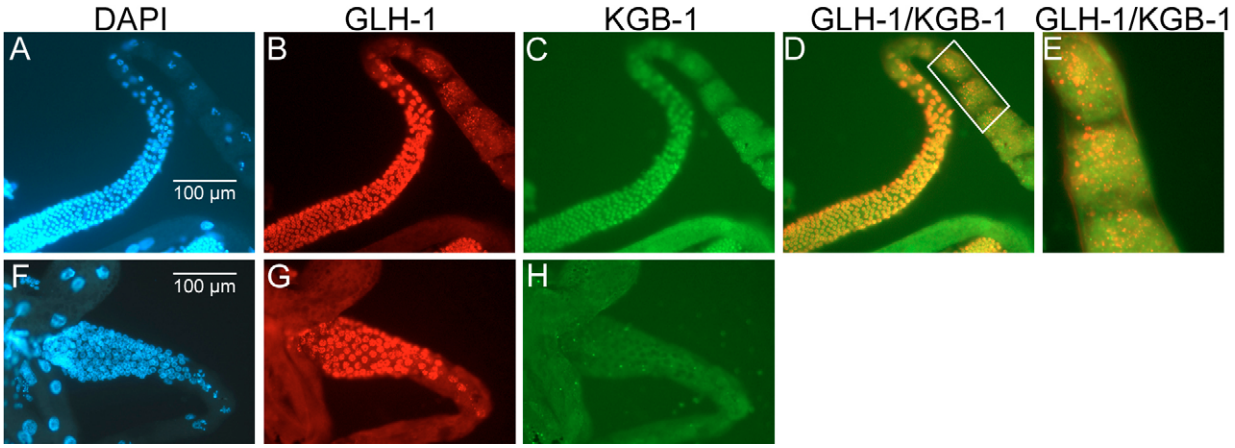

Fig. 3. KGB-1 is uniformly cytoplasmic in the distal gonad, aggregating into dispersed particles when oocytes cellularize. (**A**) A splayed gonad of a young N2 adult *C. elegans* (DAPI-stained). (**B**) The gonad in A reacted with anti-GLH-1 (red). (**C**) The gonad in A, with anti-KGB-1 (green). (**D**) A merged image of B and C. (**E**) Magnified view (1000×) of maturing oocytes (the boxed region from D). (**F**) A splayed gonad from a young *kgb-1(km21)* worm (DAPI). (**G**) The gonad in F with anti-GLH-1. (**H**) The gonad in F with anti-KGB-1. The *kgb-1(km21)* strain (Mizuno et al., 2004) was used in F-H to establish the specificity of the N-terminal KGB-1 antibody as this region is deleted in *kgb-1(km21)*, but not in *kgb-1(um3)*.

truncations of GLH-1 lacking the MAPK D site and/or the phosphodegron motif. As summarized in Fig. 4B, full-length GLH-1 bound KGB-1, as did an N-terminal truncation retaining the phosphodegron and the D site, whereas a C-terminal GLH-1 truncation, eliminating both the phosphodegron and the MAPK D site, did not bind, nor did a truncated protein in which the D site was missing but the putative phosphodegron remained. Next, we used site-directed mutagenesis to construct a deletion of the D site, as well as two point-mutated sites. As judged by GST pull-downs, neither of the point-mutated sites completely abrogated KGB-1 binding, although the K581N/L588W mutation (Fig. 4C, lane 2) bound less well than the wild-type protein and, perhaps surprisingly, the K581N/L589W mutant construct (Fig. 4C, lane 1) consistently bound with higher affinity, suggesting that sequences around the consensus might also affect binding. As predicted, the D site deletion essentially eliminated KGB-1 binding (Fig. 4C, lane 3). Thus, these results point to the importance of the MAPK D site in the binding of KGB-1 to GLH-1, but do not rule out possible involvement of other interaction sites.

KGB-1 phosphorylates GLH-1 and targets it for degradation via the proteasome

KGB-1 phosphorylates heterologous c-Jun when activated by the MAPKK, MEK-1 (Mizuno et al., 2004); however, the *C. elegans* genome does not encode a recognizable c-Jun homolog. To test whether KGB-1 can phosphorylate GLH-1, recombinant GST-tagged GLH-1 was used in kinase assays with immunoprecipitated HA-tagged KGB-1 grown in HEK293 cells that had been co-transfected with Flag-tagged MEK-1. After incubation with [γ-^{32}P]ATP, the proteins were assayed by autoradiography. On its own, KGB-1 was able to phosphorylate c-Jun and GLH-1, albeit at low levels (Fig. 5A, lane 1); however, when MEK-1 was added, phosphorylation of c-Jun and GLH-1 dramatically increased (Fig. 5A, lane 2) and when the ATP-binding site of KGB-1 was mutated (K67N), KGB-1 was unable to phosphorylate either protein (Fig. 5A, lane 3). Since KGB-1 can phosphorylate GLH-1, GLH-1 might be a KGB-1 substrate.

To determine whether KGB-1 regulates GLH-1 in a proteosome-dependent manner, GLH-1 was expressed in insect cells alone, with GST (another negative control), or with CSN-5 or KGB-1. Cells were infected with recombinant baculovirus, grown for 18 hours, and then treated with the proteasome inhibitor MG132 for 5 hours; GLH-1 levels were then examined (Fig. 5B). When expressed alone, or with either GST or CSN-5, GLH-1 accumulated to high levels, both with and without MG132 (Fig. 5B, lanes 1-4 and 7-8). By contrast, co-expression of GLH-1 with KGB-1 resulted in greatly reduced GLH-1 levels (Fig. 5B, lane 6); however, when the proteasome was blocked, GLH-1 levels increased during the last 5 hours of infection (Fig. 5B, lane 5). These results suggest that KGB-1 targets GLH-1 for degradation by the proteasome.

Table 1. GLH-1, CSN-5 and Vasa contain consensus motifs used by MAP kinases

	MAPK docking (D) sites	Phosphodegron site
Consensus	K/R-X-X/K/R-K/R-X(1-4)-L/I-X-L/I or K/R-K/R-K/R-X(1-5)-L/I-X-L/I	I/L-I/L/P-pT-P-notK/R
GLH-1 (aa 581)	KKDKLLEL consensus	GLH-1 (aa 423) ILTPT consensus
GLH-4 (aa 977)	KRD**A**IYKLLGI	GLH-4 (aa 820) I**V**APT
GLH-4 (aa 977)	KR**D**AIYKLLGI	GLH-4 (aa 758) R**P**TPI
CSN-5 (aa 54)	KQIKISAIAL consensus	Vasa (aa 267) IPTPI consensus
Vasa (aa 475)	KRSKLIEI consensus	

Amino acids matching putative consensus motifs are underlined; those in bold are non-consensus and those unmarked are amino acids not discriminatory for the MAPK D motif. Variations of the D site consensus have been reported, with GLH-1 matching one, and GLH-4 having one mismatch for either of two shown. CSN-5 has a consensus D site, as does Vasa. Both GLH-1 and Vasa have consensus phosphodegrons; although GLH-4 has two potential sites, neither is consensus. PGL-1 has no D site, nor a phosphodegron (not shown). Sequences were aligned using the NCBI BLAST program (bl2seq blastp).

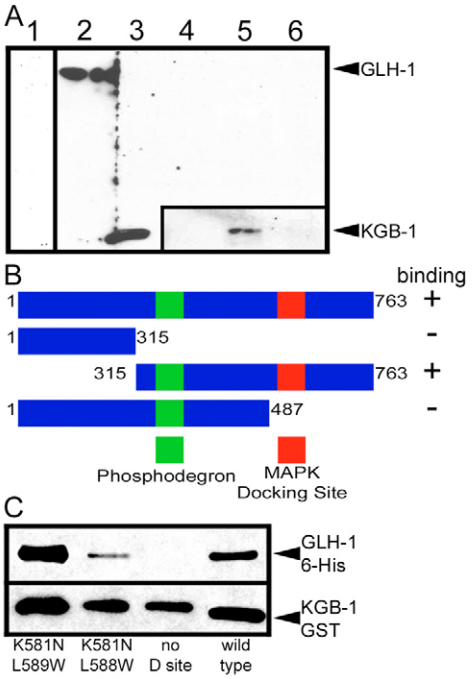

Fig. 4. Interactions of KGB-1 and GLH-1. (**A**) Pull-down analysis. Lane 1, input *kgb-1(um3)* homogenate with anti-KGB-1 (C2-2) antibodies. Lane 2, input *kgb-1(um3)* homogenate, with anti-GLH-1. Lane 3, input N2 protein, with anti-KGB-1. Lane 4, N2 homogenate incubated with GST protein and GST beads, with anti-KGB-1. Lane 5, N2 homogenate incubated with GLH-1-GST and GST beads; reacted with anti-KGB-1. Lane 6, *kgb-1(um3)* homogenate incubated with GLH-1-GST and GST beads; reacted with anti-KGB-1. Lanes 4-6 are shown at a longer exposure than lanes 1-3, as the KGB-1 pulled down by GLH-1 was considerably less than the total KGB-1 in *C. elegans*, lane 3. (**B**) A schematic of 6-His-tagged GLH-1 constructs, with binding indicated (+). (**C**) Pull-down analysis. KGB-1-GST with GLH-1-6-His and three mutants of GLH-1, each tagged with 6-His. Lane 1, His-tagged GLH-1-K581N/L589W with KGB-1-GST. Lane 2, 6-His-tagged GLH-1-K581N/L588W with KGB-1-GST. Lane 3, 6-His-tagged GLH-1 lacking the D site (missing aa 581-588) with KGB-1-GST (on long exposures, GLH-1 is seen to weakly bind KGB-1, not shown). Lane 4, KGB-1-GST and full-length, wild-type GLH-1-6-His.

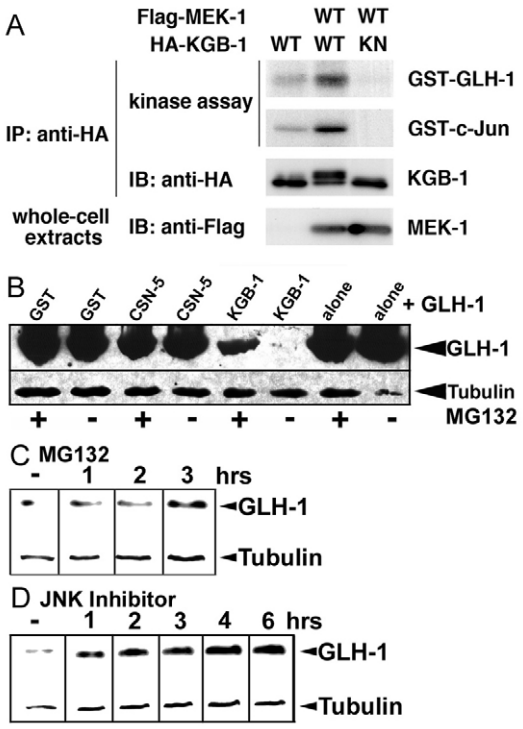

Fig. 5. KGB-1 can phosphorylate GLH-1; proteosomal or JNK inhibitors increase GLH-1. (**A**) In vitro kinase reactions were carried out with GLH-1-GST (first row) and c-Jun-GST (second row). Inputs of KGB-1 (third row) and MEK-1 (fourth row), both with HA tags, are shown. In lane 1, basal levels of GLH-1 or c-Jun phosphorylation occur when incubated with KGB-1 alone. Lane 2 shows phosphorylation levels of GLH-1 and c-Jun when KGB-1 is activated by MEK-1. A mutated inactive form of KGB-1 was used in lane 3. (**B**) HighFive cells were infected with GLH-1-6-His and KGB-1-GST (lanes 5 and 6), GLH-1-6-His and GST alone (lanes 1 and 2), GLH-1-6-His and CSN-5-GST (lanes 3 and 4) or 6-His-tagged GLH-1 alone (lanes 7 and 8) and grown for 18 hours. They were then treated (or not) with 1 μM MG132 and grown an additional 5 hours before lysing. GLH-1 levels were measured with anti-His antibody. A β-tubulin loading control is shown. (**C**) Young N2 adult *C. elegans* were grown in liquid culture for 6 hours, with 1 μM M6132 added for 0-3 hours; GLH-1 levels were assayed by western blot with an α-tubulin loading control. (**D**) Under the same conditions as in C, 50 μM SP600125 was added and GLH-1 tested by western blot, again with an α-tubulin control.

To assess whether either MG132 or the JNK inhibitor SP600125 could be used in live worms, we incubated wild-type *C. elegans* with these chemicals at concentrations shown to be effective in vitro and then tested these worms for changes in GLH-1 levels. When live worms were exposed to MG132 for 3 hours, the GLH-1 levels increased over 3-fold, with an average increase of 3.4-fold in three trials (Fig. 5C). We also chose to test the effect of the JNK inhibitor SP600125, as it would be likely to be more specific and potentially less toxic to worms than MG132. After 3 hours incubation with SP600125, GLH-1 levels increased more than 4-fold beyond those of untreated controls, with an average increase of 4.6 in three independent experiments (Fig. 5D), indicating that blocking either the proteosome or the specific JNK activity of KGB-1 (and that of the other two *C. elegans* JNK proteins, JNK-1 and KGB-2) results in a relatively rapid accumulation of GLH-1. Therefore, the regulation of GLH-1 seen with the *kgb-1* mutant can be mimicked with inhibitors, both in vitro and in vivo.

Knocking down GLH-1 levels partially rescues *kgb-1* sterility

To address whether increased levels of GLH-1 contribute to sterility in *kgb-1* worms, GLH-1 levels were knocked down in *kgb-1* by RNAi. Young adult N2 and *kgb-1* worms grown at the permissive temperature were injected with *glh-1* dsRNA, shifted to 26°C and purged of pre-existing progeny (Table 2). F_1 progeny were then tested for production of any F_2 offspring. Under these conditions, *glh-1(RNAi)* into N2 resulted in only 4% of the F_1 worms producing any offspring, whereas *glh-1(RNAi)* into *kgb-1* resulted in 20% of the F_1 progeny producing one or more offspring. This contrasts with the uninjected controls, where 99% of the N2 worms and 12% of the *kgb-1* mutants had at least one F_2. To control for the possibility that *kgb-1(um3)* mutants might be defective in RNAi, dsRNAs corresponding to the ubiquitously expressed *C. elegans actin* genes and to *pan-1*, a novel gene with germline-enriched expression (Gao et al., 2006) (G. Gao and K.L.B., unpublished) were also tested in

Table 2. Effect of *glh-1(RNAi)* on fertility of wild-type and *kgb-1(um3)* worms

Strain	Number F_1s tested	% Fertile F_1s	*P* value
N2 uninjected	105	99	Versus *kgb-1* uninjected, $P>1\times10^{-10}$
kgb-1 uninjected	116	12	Versus *kgb-1; glh-1(RNAi)*, $P>0.05$
N2 with *glh-1(RNAi)*	476	4	Versus *kgb-1; glh-1(RNAi)*, $P>3\times10^{-5}$
kgb-1; glh-1(RNAi)	288	20	

glh-1(RNAi) was performed into N2 and *kgb-1* young adults at 20°C. The worms were shifted to 26°C and purged of maternal protein. Resulting F_1s were individually plated. Worms with any viable progeny were considered fertile.

the *kgb-1* background; no significant differences between N2s and *kgb-1* were found for these RNAs (Table 3). Thus, *kgb-1* is not defective in RNAi and whereas fertility is only partially restored by *glh-1(RNAi)* into *kgb-1* mutants (Table 2), the removal of excess GLH-1 results in significantly more fertile animals ($P<0.05$). Therefore, by reducing GLH-1 levels in *kgb-1* worms, some mutant animals are rescued, perhaps indicating that elevated GLH-1 levels are detrimental to reproduction. The lack of complete rescue might reflect the variable amount of GLH-1 removed by this technique; alternatively, it could also imply that KGB-1 has other, as yet undetermined targets in the *C. elegans* germline.

Perhaps also supporting the hypothesis that increased GLH-1 levels are deleterious, we found that when post-reproductive (4 days beyond L4 at 20°C) *kgb-1* hermaphrodites were mated with N2 males, they produced less than a third as many additional progeny as did mated N2s of the same age. Each *kgb-1* had an average of 23 more progeny ($n=7$), whereas the N2s produced 83 ($n=11$). Therefore, keeping GLH levels low after hermaphrodites have depleted their own sperm may enhance fertility upon mating. The *glh-1(RNAi)* and mating experiments imply that excess GLH-1 has negative consequences for reproduction. We have attempted to test this hypothesis directly by producing an overexpressing GLH-1 transgenic line, with no success. Although our inability to produce this overexpressing strain is not definitive, it might also imply that too much GLH-1 is detrimental to fertility in *C. elegans.*

CSN-5 also regulates GLH-1 levels

CSN-5 and the COP9 signalosome complex associate with several kinases. In mammals, protein kinase CK2 (also known as PCK2 – Human Gene Nomenclature Database) and PKD (also known as PRKD1) and inositol 1,3,4-triphosphate 5/6 kinase associate with the CSN complex, whereas the *C. elegans* interactome project reported that the MAP kinases MPK-1, PMK-1 and PMK-2 bind CSN-5 (Li et al., 2004; Sun et al., 2002; Uhle et al., 2003). To determine whether KGB-1 associates with CSN-5, we again used GST pull-down analyses and found that KGB-1 binds CSN-5 (Fig. 6A, lane 2), the first JNK reported to do so. This interaction is robust, withstanding high salt (300 mM LiCl) stringency (data not shown). CSN-5, like GLH-1, has a consensus D site (Table 1), perhaps facilitating the binding of KGB-1 to CSN-5.

Since CSN-5 and KGB-1 bind one another and bind GLH-1 in vitro and in vivo (this report) (Smith et al., 2002), we investigated whether loss of CSN-5 would affect KGB-1 function. After *csn-5(RNAi)* into N2, only 25% of the injected worms produced any fertile F_1 progeny; by contrast, *csn-5(RNAi)* into *kgb-1* resulted in 63% of the *kgb-1* worms producing a few fertile F_1 progeny (Table 3), a highly significant difference ($P<1\times10^5$). Therefore, fertility improves in *kgb-1* worms when *csn-5* is also missing (or reduced), implying a functional interaction between KGB-1 and CSN-5 in *C. elegans.*

To test whether the rescue seen for the fertile *kgb-1; csn-5(RNAi)* worms (Table 3) is due to an equilibration of GLH-1 levels, in effect balancing the roles of two proteins with opposing actions, we compared GLH-1 levels in *kgb-1; csn-5(RNAi)* fertile animals with uninjected N2s and uninjected *kgb-1*s (Fig. 6B). We found that the fertile *kgb-1*; *csn-5(RNAi)* worms had GLH-1 levels that were, on average, 2.8-fold lower than their uninjected *kgb-1* siblings (lane 3 versus lane 2) and these levels were closer to those of aged-matched wild-type animals (lane 1). The results presented in Fig. 6B suggest that KGB-1 and CSN-5 work in opposition to control GLH-1 levels. Perhaps, when KGB-1 is not present to target GLH proteins for degradation, the protective role of CSN-5 might be less necessary.

Vasa interacts with KGB-1 and CSN-5

In searching for D sites and phosphodegrons, we discovered that Vasa, the well-studied *Drosophila* polar granule component, also contains consensus sites for each (Table 1). In fact, GLH-1/Vasa orthologs in many species contain docking sites and phosphodegrons (not shown). Therefore, we tested whether Vasa might interact with KGB-1 or CSN-5 when co-expressed in insect cells. We cloned *vas* into the pFastBac vector, adding either a 6-His tag or a GST tag to the full-length *vas* cDNA (Hay et al., 1988a). The His-tagged Vasa construct was co-expressed with KGB-1 or with

Table 3. *kgb-1* is RNAi-sensitive; *csn-5(RNAi)* indicates that KGB-1 and CSN-5 interact

dsRNA injected into:	Number of worms injected	Number with RNAi effect in all F_1s	Number F_1s without RNAi effect	% F_1s with RNAi effect
actin into N2	23	19	4*	83
actin into *kgb-1*	21	19	2*	90
pan-1 into N2	24	20†	4‡	83
*pan-1*into *kgb-1*	26	24†	2‡	92
csn-5 into N2	63	47	16§	75
csn-5 into *kgb-1*	63	23	40§	37

For RNAi, N2 or *kgb-1* young adults at 20°C were injected, individually plated and purged of maternal protein. For *actin* and *pan-1(RNAi)*, injected worms were scored for producing dead eggs (*actin*) or arrested L2-sized larvae (*pan-1*) 3 days after injection. Student's *t*-tests of differences between N2 and *kgb-1* are highly significant for *csn-5* ($P<1\times10^{-5}$); with no significant differences between N2 and *kgb-1* for *actin* or *pan-1,* indicating *kgb-1(um3)* is not RNAi defective.
*Injected nematodes designated as *actin* 'escapers' had 1-2 live progeny that grew to fertile adults.
†One *pan-1*-injected N2 and one *pan-1*-injected *kgb-1* became sterile adults and were included with those showing RNAi effects.
‡*pan-1* 'escapers' had 1-2 larvae that became fertile adults.
After *csn-5(RNAi)*, F_1s were scored on day 5-6 as producing no F_2 or §producing one (or more) F_2s.

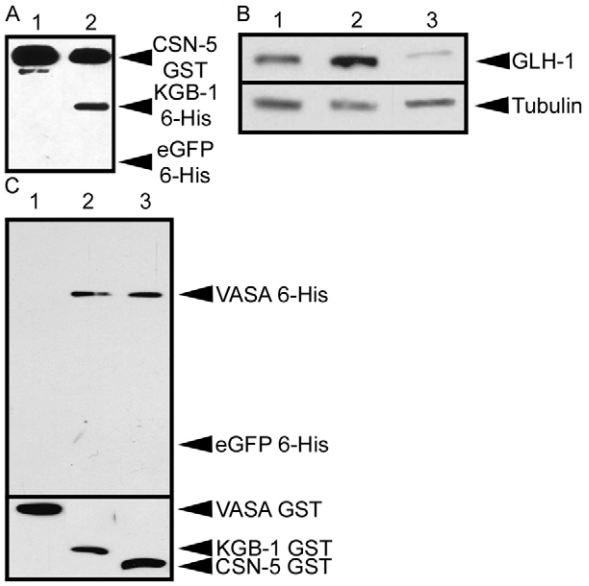

Fig. 6. Biochemical and genetic interactions between *C. elegans* KGB-1 and CSN-5; *Drosophila* Vasa interacts with KGB-1 and CSN-5. (**A**) GST pull-downs using CSN-5-GST and KGB-1-6-His. Lane 1, CSN-5-GST with eGFP-6-His, negative control (the smaller band is likely to be a CSN-5 breakdown product). eGFP size indicated. Lane 2, CSN-5-GST with KGB-1-6-His. (**B**) After *csn-5(RNAi)* in *kgb-1*, GLH-1 was assayed by western blot using 30 worms/lane of: lane 1, uninjected N2 worms; lane 2, uninjected *kgb-1* mutants; lane 3, fertile F1 progeny of *csn-5(RNAi)* into *kgb-1*. All worms assayed were ~3d>L4 stage, 20°C. F_1 worms were picked as adults 5-6 days after moving mothers to fresh plates to eliminate eggs formed before injection (purging). This experiment was repeated four times, with the decrease in GLH-1 for the fertile *kgb-1*; *csn-5(RNAi)* animals averaging 2.8-fold lower than their *kgb-1* uninjected siblings (range 1.6-5.3) (lane 3 versus lane 2). This difference is statistically significant, $P<0.03$. β-tubulin served as a loading control. (**C**) Baculoviral co-infections of insect cells treated as in Fig. 4B,C. Lane 1, Vasa-GST with eGFP-6-His; lane 2, Vasa-6-His with KGB-1-GST; lane 3, Vasa-6-His with CSN-5-GST. The His-tagged proteins pulled down are shown in the upper panel, with the GST proteins shown below. Input proteins for these pull-down assays are shown in Fig. S3 in the supplementary material.

CSN-5, both tagged with GST. Whereas the Vasa-GST did not pull down eGFP (Fig. 6C, lane 1), GST-tagged KGB-1 and CSN-5 pulled down Vasa 6-His (Fig. 6C, lanes 2 and 3). Thus, *Caenorhabditis* proteins KGB-1 and CSN-5 recognize and bind to the *Drosophila* Vasa germ granule protein.

DISCUSSION

The GLH P granule components are crucial to a fertile *C. elegans* germline. Two proteins, KGB-1, a MAP kinase, and CSN-5, a subunit of the COP9 signalosome, that were first found to bind the GLHs in a two-hybrid screen, are also essential for fertility. Here, additional GLH-1, KGB-1 and CSN-5 interactions indicate that KGB-1 and CSN-5 act in opposition to control the degradation of GLH-1. We came to this conclusion through both in vitro analyses, including pull-downs and inhibitor studies with proteins co-expressed in baculovirus, and in vivo experiments using western blot analysis, immunocytochemistry, pull-downs from worm lysates, functional interactions using mutant strains combined with RNAi and inhibitor studies in live worms. To summarize, in *kgb-1(um3)* worms, levels of GLH-1 are higher than normal and the morphology of GLH-1 in P granules is disrupted. In wild-type germlines, GLH-1 and KGB-1 overlap in location during mitosis and through the pachytene stage of meiosis before dispersing into discrete puncta in maturing oocytes. KGB-1 and CSN-5 bind one another in pull-down assays and each binds GLH-1; in addition, KGB-1 requires a MAPK-docking site to bind GLH-1, and KGB-1 phosphorylates and targets GLH-1 for degradation via the proteosome. Inhibitor studies in live worms substantiate the in vitro results. We also report that *csn-5(RNAi)* into *kgb-1(um3)* mutants ameliorates the sterile phenotype of *kgb-1* worms, producing greater numbers of fertile offspring, concomitant with changes in GLH-1 levels back to near normal in the rare *kgb-1; csn-5(RNAi)* fertile worms. Thus, by multiple indicators, KGB-1 and CSN-5 act together to target and protect GLH-1. By maintaining appropriate levels of GLH-1, we propose this partnership contributes to homeostasis in the *C. elegans* germline and results in fertility. The *C. elegans* CSN-5 and KGB-1 proteins bind to *Drosophila* Vasa; thus, the opposing mechanisms reported here could be conserved from worms to flies.

Why GLH-1 levels might be important for germline homeostasis

Homeostasis in the germline has been very convincingly shown to balance numbers of primordial germ cells (PGCs) with those of intermingled somatic cells in the *Drosophila* ovary (Gilboa and Lehmann, 2006). In *C. elegans*, we report a homeostatic regulation of GLH-1 that appears necessary for reproductive success. Regulation of GLH-1 by KGB-1 could ensure continued fertility by removing excess GLH-1 protein as *C. elegans* become post-reproductive; in addition, KGB-1 may remove excess GLH-1 from those germ cells undergoing apoptosis during pachytene (Gumienny et al., 1999). Phosphorylation of GLH-1 by KGB-1 could be the signaling event that removes GLH-1 (and the P granules) from their peri-nuclear location. There are precedents for a protein both changing the location of its target and being involved in its degradation; for example, several of us have recently reported that *C. elegans* RLE-1, an E3 ligase, has such an effect on DAF-16 (Li et al., 2007).

The KGB-1 signaling pathway might be complex

Previous work has shown that KGB-1 is activated by the MAPKK, MEK-1 (Mizuno et al., 2004), yet we found that loss of MEK-1 leads to a much less robust accumulation of GLH-1 protein than does the loss of KGB-1 (W.L. and K.L.B., unpublished). This suggests that alternate MAPK pathways, perhaps including the SEK-1/PMK-1 p38-type MAPK pathway (Mizuno et al., 2004), might influence the activity of KGB-1, broadening the signals to which KGB-1 is receptive and adding to its potential responsiveness. KGB-2, a protein very similar to KGB-1, only appears to have a small role in regulating the GLH proteins, as *kgb-1; kgb-2* double mutants show only slightly higher GLH-1 levels than *kgb-1* alone (W.L. and K.L.B., unpublished). Therefore, in regulating GLH-1, KGB-1 and KGB-2 might function redundantly or in parallel pathways and KGB-2 might respond to as yet unrecognized stimuli. Although we expect that GLH-1 is a major target of KGB-1, as the rescue of *kgb-1* by *glh-1(RNAi)* is only a partial return to fertility, it is possible that KGB-1 has additional germline targets that remain to be discovered. It is not surprising that KGB-1, a MAP kinase, may be regulated by multiple MAPKKs and/or may recognize multiple target substrates, as most MAP kinases participate in complex cross-talk with various signaling pathways. In addition to KGB-1 and CSN-5, the GLHs are also likely to respond to multiple regulators, including transcription factors. Both N2 and *kgb-1* worms show a

decrease in GLH-1 protein as they age (Fig. 1B,D); perhaps *glh-1* mRNA levels decline in post-reproductive worms, contributing to the regulation of GLH-1. However, this report identifies GLH-1 as a likely target of the KGB-1 MAP kinase and demonstrates dramatic consequences for the *C. elegans* germline when the KGB-1/GLH-1 relationship is disrupted.

CSN-5 as a protective partner

In *C. elegans*, CSN-5 has been shown to target MEI-1 for degradation (Pintard et al., 2003); our report is the first to implicate CSN-5 in a protective role in *C. elegans*. We report that CSN-5 contains a conserved MAPK D site and that CSN-5 interacts both physically and genetically with KGB-1. The suggestion of a protective role for CSN-5 regarding GLH-1 is also based on other researchers reporting a protective role for the mammalian CSN-5 homolog, which protects c-Jun, Id1 and Id3, as well as our finding that loss of *C. elegans* CSN-5 closely mimics loss of GLH-1 and GLH-4 (Berse et al., 2004; Naumann et al., 1999; Smith et al., 2002).

A working model

A parsimonious explanation for the relationship between GLH-1, KGB-1 and CSN-5 that takes into account the results presented here would be that CSN-5 antagonizes KGB-1 function, as shown in the model (Fig. 7), with KGB-1 ultimately targeting GLH-1 for proteasomal degradation by binding at the D site and using the phosphodegron motif as a phosphorylation site.

Are GLH and Vasa homologs regulated by similar homeostatic mechanisms?

Homologs of Vasa or GLH-like (DEAD-box proteins that have CCHC zinc fingers) proteins are present in most if not all animals in which germ granules have been studied, making this protein family the most highly conserved germline determinant. We have shown here the MAPK D site is necessary for the interaction of GLH-1 with KGB-1. In the myriad of Vasa and GLH homologs, both the D site and the phosphodegron motif are often present (Table 1 and data not shown). We also find that *Drosophila* Vasa binds to both CSN-5 and KGB-1 in pull-down assays (Fig. 6C). These results suggest that *Drosophila* CSN5 and perhaps the closely related *Drosophila* BSK protein might have a relationship with Vasa similar to that reported here for GLH-1 with CSN-5 and KGB-1. Thus, GLH and Vasa-like proteins might be regulated by degradation in many species, ensuring homeostasis by monitoring germ granule integrity and maintaining proper levels of crucial germline components.

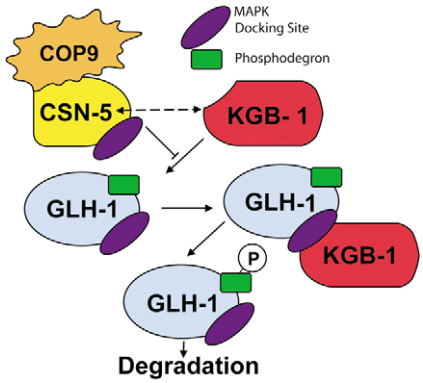

Fig. 7. Model of possible interactions of KGB-1 and CSN-5 with GLH-1 in *C. elegans*. This model is based on data presented here, which suggest that CSN-5 protects GLH-1 from degradation. The MAPK docking site in GLH-1 is important for GLH-1/KGB-1 interactions. Kinase assays show that KGB-1 can phosphorylate GLH-1, perhaps at the conserved phosphodegron motif. In addition, GLH-1, CSN-5 and KGB-1 physically and functionally interact to allow cross-talk between CSN-5 and KGB-1, with CSN-5 antagonizing KGB-1 function and protecting GLH-1. While interacting with KGB-1 and GLH-1, CSN-5 might associate with the COP9 signalosome.

We thank Dr Susan Strome (Indiana University) for anti-PGL-1 and additional anti-GLH-1 antibodies and Dr Bruce Hay (while in the Jan laboratory, UCSF) for the full-length *vas* cDNA. From the University of Missouri (MU) we thank Dr Pliny Smith for initiating these studies, Dr Mark Hannink for helpful advice and Ge Gao for providing the *actin* and *pan-1* dsRNAs. A.M.O. and T.J.M. were supported by MU Life Sciences Fellowships and A.M.O. received support from NIH training grant NIGMS2T32GM08396-11. Funding was provided by a National Science Foundation grant NSF IBN 0415699 to K.L.B.

Supplementary material

Supplementary material for this article is available at
http://dev.biologists.org/cgi/content/full/134/18/3383/DC1

References

Adachi-Yamada, T., Fujimura-Kamada, K., Nishida, Y. and Matsumoto, K. (1999). Distortion of proximodistal information causes JNK-dependent apoptosis in *Drosophila* wing. *Nature* **400**, 166-169.

Bech-Otschir, D., Kraft, R., Huang, X., Henklein, P., Kapelari, B., Pollmann, C. and Dubiel, W. (2001). COP9 signalosome-specific phosphorylation targets p53 to degradation by the ubiquitin system. *EMBO J.* **20**, 1630-1639.

Berse, M., Bounpheng, M., Huang, X., Christy, B., Pollmann, C. and Dubiel, W. (2004). Ubiquitin-dependent degradation of Id1 and Id3 is mediated by the COP9 signalosome. *J. Mol. Biol.* **343**, 361-370.

Bosch, M., Serras, F., Martin-Blanco, E. and Baguna, J. (2005). JNK signaling pathway required for wound healing in regenerating *Drosophila* wing imaginal discs. *Dev. Biol.* **280**, 73-86.

Chamovitz, D. A. and Glickman, M. (2002). The COP9 signalosome. *Curr. Biol.* **12**, R232.

Church, D. L., Guan, K.-L. and Lambie, E. J. (1995). Three genes of the MAP kinase cascade, *mek-2*, *mpk-1/sur-1* and *let-60 ras*, are required for meiotic cell cycle progression in *Caenorhabditis elegans*. *Development* **121**, 2525-2535.

Cope, G. A. and Deshaies, R. J. (2003). COP9 signalosome: a multifunctional regulator of SCF and other cullin-based ubiquitin ligases. *Cell* **114**, 663-671.

DeRenzo, C., Reese, K. J. and Seydoux, G. (2003). Exclusion of germ plasm proteins from somatic lineages by cullin-dependent degradation. *Nature* **424**, 685-689.

Epstein, H. F. and Shakes, D. C. (1995). *Caenorhabditis elegans: Modern Biological Analysis of an Organism* (*Methods in Cell Biology*). San Diego: Academic Press.

Gao, G., Raikar, S., Davenport, B., Mutapcic, L., Montgomery, R., Kuzmin, E. and Bennett, K. L. (2006). Cross-species RNAi: selected *Ascaris suum* dsRNAs can sterilize *Caenorhabditis elegans*. *Mol. Biochem. Parasitol.* **146**, 124-128.

Gilboa, L. and Lehmann, R. (2006). Soma-germline interactions coordinate homeostasis and growth in the *Drosophila* gonad. *Nature* **443**, 97-100.

Gruidl, M. E., Smith, P. A., Kuznicki, K. A., McCrone, J. S., Kirchner, J., Strome, S. and Bennett, K. L. (1996). Multiple potential germline helicases are components of the germline-specific P granules of *Caenorhabditis elegans*. *Proc. Natl. Acad. Sci. USA* **93**, 13837-13842.

Gumienny, T. L., Lambie, E., Hartwieg, E., Horvitz, H. R. and Hengartner, M. O. (1999). Genetic control of programmed cell death in the *Caenorhabditis elegans* hermaphrodite germline. *Development* **126**, 1011-1022.

Hay, B., Ackerman, L., Barbel, S., Jan, L. Y. and Jan, Y. N. (1988a). Identification of a component of *Drosophila* polar granules. *Development* **103**, 625-640.

Hay, B., Jan, L. Y. and Jan, Y. N. (1988b). A protein component of *Drosophila* polar granules is encoded by *vasa* and has extensive sequence similarity to ATP-dependent helicases. *Cell* **55**, 577-587.

Huffman, D. L., Abrami, L., Sasik, R., Corbeil, J., van der Goot, F. G. and Aroian, R. V. (2004). Mitogen-activated protein kinase pathways defend against bacterial pore-forming toxins. *Proc. Natl. Acad. Sci. USA* **101**, 10995-20000.

Igaki, T., Kanda, H., Yamamoto-Goto, Y., Kanuka, H., Kuranaga, E., Aigaki, T. and Miura, M. (2002). Eiger, a TNF superfamily ligand that triggers the *Drosophila* JNK pathway. *EMBO J.* **21**, 3009-3018.

Ip, Y. T. and Davis, R. J. (1998). Signal transduction by the c-Jun N-terminal kinase (JNK) – from inflammation to development. *Curr. Opin. Cell Biol.* **10**, 205-219.

Jacinto, A., Woolner, S. and Martin, P. (2002). Dynamic analysis of dorsal closure in *Drosophila*: from genetics to cell biology. *Dev. Cell* **3**, 9-19.

Jacobs, D., Glossip, D., Xing, H., Muslin, A. J. and Kornfeld, K. (1999).

Multiple docking sites on substrate proteins form a modular system that mediates recognition by ERK MAP kinase. *Genes Dev.* **13**, 163-175.
Jones, A. R., Francis, R. and Schedl, T. (1996). GLD-1, a cytoplasmic protein essential for oocyte differentiation, shows stage- and sex-specific expression during *Caenorhabditis elegans* germline development. *Dev. Biol.* **180**, 165-183.
Kawasaki, I., Shim, Y. H., Kirchner, J., Kaminker, J., Wood, W. B. and Strome, S. (1998). PGL-1, a predicted RNA-binding component of germ granules, is essential for fertility in *C. elegans*. *Cell* **94**, 635-645.
Koga, M., Zwaal, R., Guan, K. L., Avery, L. and Ohshima, Y. (2000). A *Caenorhabditis elegans* MAP kinase kinase, MEK-1, is involved in stress responses. *EMBO J.* **19**, 5148-5156.
Kuznicki, K. A., Smith, P. A., Leung-Chiu, W. M., Estevez, A. O., Scott, H. C. and Bennett, K. L. (2000). Combinatorial RNA interference indicates GLH-4 can compensate for GLH-1; these two P granule components are critical for fertility in *C. elegans*. *Development* **127**, 2907-2916.
Lasko, P. F. and Ashburner, M. (1988). The product of the *Drosophila* gene *vasa* is very similar to eukaryotic initiation factor-4A. *Nature* **335**, 611-617.
Li, S., Liu, X. and Ascoli, M. (2000). p38JAB1 binds to the intracellular precursor of the lutropin/choriogonadotropin receptor and promotes its degradation. *J. Biol. Chem.* **275**, 13386-13393.
Li, S., Armstrong, C. M., Bertin, N., Ge, H., Milstein, S., Boxem, M., Vidalain, P. O., Han, J. D., Chesneau, A., Hao, T. et al. (2004). A map of the interactome network of the metazoan *C. elegans*. *Science* **303**, 540-543.
Li, W., Gao, B., Lee, S.-M., Bennett, K. and Fang, D. (2007). RLE-1, an E3 ubiquitin ligase, regulates *C. elegans* aging by catalyzing DAF-16 polyubiquitination. *Dev. Cell* **12**, 1-12.
Mattila, J., Omelyanchuk, L., Kyttälä, S., Turunen, H. and Nokkala, S. (2005). Role of Jun N-terminal kinase (JNK) signaling in the wound healing and regeneration of a *Drosophila melanogaster* wing imaginal disc. *Int. J. Dev. Biol.* **49**, 391-399.
McCarter, J., Bartlett, B., Dang, T. and Schedl, T. (1999). On the control of oocyte meiotic maturation and ovulation in *Caenorhabditis elegans. Dev. Biol.* **205**, 111-128.
Miller, M. A., Nguyen, V. Q., Lee, M.-H., Kosinski, M., Schedl, T., Caprioli, R. M. and Greenstein, D. (2001). A sperm cytoskeletal protein that signals ooctye meiotic maturation and ovulation. *Science* **291**, 2144-2147.
Mizuno, T., Hisamoto, N., Terada, T., Kondo, T., Adachi, M., Nishida, E., Kim, D. H., Ausubel, F. M. and Matsumoto, K. (2004). The *Caenorhabditis elegans* MAPK phosphatase VHP-1 mediates a novel JNK-like signaling pathway in stress response. *EMBO J.* **23**, 2226-2234.
Naumann, M., Bech-Otschir, D., Huang, X., Ferrell, K. and Dubiel, W. (1999). COP9 signalosome-directed c-Jun activation/stabilization is independent of JNK. *J. Biol. Chem.* **274**, 35297-35300.
Navarro, R. E., Shim, E. Y., Kohara, Y., Singson, A. and Blackwell, T. K. (2001). cgh-1, a conserved predicted RNA helicase required for gametogenesis and protection from physiological germline apoptosis in C. elegans. *Development* **128**, 3221-3232.
Nelson, G. A., Lew, K. K. and Ward, S. (1978). Intersex, a temperature-sensitive mutant of the nematode *Caenorhabditis elegans*. *Dev. Biol.* **66**, 386-409.
Nishi, Y. and Lin, R. (2005). DYRK2 and GSK-3 phosphorylate and promote the timely degradation of OMA-1, a key regulator of the oocyte-to-embryo transition in *C. elegans*. *Dev. Biol.* **288**, 139-149.
Olmstead, J. B. (1986). Analysis of cytoskeletal structures using blot purified monospecific antibodies. *Methods Enzymol.* **134**, 467-472.
Orlicky, S., Tang, X., Willems, A., Tyers, M. and Sicheri, F. (2003). Structural basis for phosphodependent substrate selection and orientation by the SCF Cdc4 ubiquitin ligase. *Cell* **112**, 243-256.
Page, B. D., Guedes, S., Waring, D. and Priess, J. R. (2001). The *C. elegans* E2F- and DP-related proteins are required for embryonic asymmetry and negatively regulate Ras/MAPK signaling. *Mol. Cell* **7**, 451-460.
Pellettieri, J., Reinke, V., Kim, S. K. and Seydoux, G. (2003). Coordinate activation of maternal protein degradation during the egg-to-embryo transition in *C. elegans*. *Dev. Cell* **5**, 451-462.
Pintard, L., Kurz, T., Glaser, S., Willis, J. H., Peter, M. and Bowerman, B. (2003). Neddylation and deneddylation of CUL-3 is required to target MEI-1/katanin for degradation at the meiosis-to-mitosis transition in *C. elegans*. *Curr. Biol.* **13**, 911-921.
Pitt, J. N., Schisa, J. A. and Priess, J. R. (2000). P granules in the germ cells of *Caenorhabditis elegans* adults are associates with clusters of nuclear pores and contain RNA. *Dev. Biol.* **219**, 315-333.
Reese, K. J., Dunn, M. A., Waddle, J. A. and Seydoux, G. (2000). Asymmetric segregation of PIE-1 in *C. elegans* is mediated by two complementary mechanisms that act through separate PIE-1 protein domains. *Mol. Cell* **6**, 445-455.
Reinke, V., Smith, H. E., Nance, J., Wang, J., Van Doren, C., Begley, R., Jones, S. J., Davis, E. B., Scherer, S., Ward, S. et al. (2000). A global profile of germline gene expression in *C. elegans*. *Mol. Cell* **6**, 605-616.
Robinson, M. J. and Cobb, M. H. (1997). Mitogen-activated protein kinase pathways. *Curr. Opin. Cell Biol.* **9**, 180-186.
Roussell, D. L. and Bennett, K. L. (1993). *glh-1*: a germline putative RNA helicase from *Caenorhabditis* has four zinc fingers. *Proc. Natl. Acad. Sci. USA* **90**, 9300-9304.
Schwechheimer, C., Serino, G., Callis, J., Crosby, W. L., Lyapina, S., Deshaies, R. J., Gray, W. M., Estelle, M. and Deng, X. W. (2001). Interactions of the COP9 signalosome with the E3 ubiquitin ligase SCFTIRI in mediating auxin response. *Science* **292**, 1379-1382.
Sharrocks, A. D., Yang, S. H. and Galanis, A. (2000). Docking domains and substrate-specificity determination for MAP kinases. *Trends Biochem. Sci.* **25**, 448-453.
Shirayama, M., Soto, M. C., Ishidate, T., Kim, S., Nakamura, K., Bei, Y., van den Heuvel, S. and Mello, C. C. (2006). The conserved kinases CDK-1, GSK-3, KIN-19, and MBK-2 promote OMA-1 destruction to regulate the oocyte-to-embryo transition in *C. elegans*. *Curr. Biol.* **16**, 47-55.
Smith, P. A., Leung-Chiu, W. M., Montgomery, R., Orsborn, A., Kuznicki, K. A., Gressman-Coberly, E., Mutapcic, L. and Bennett, K. L. (2002). The GLH proteins, *Caenorhabditis elegans* P granule components, associate with CSN-5 and KGB-1, proteins necessary for fertility, and with ZYX-1, a predicted cytoskeletal protein. *Dev. Biol.* **251**, 333-347.
Stitzel, M. L., Pellettieri, J. and Seydoux, G. (2006). The *C. elegans* DYRK kinase MBK-2 marks oocyte proteins for degradation in response to meiotic maturation. *Curr. Biol.* **16**, 56-62.
Strome, S. and Wood, W. B. (1982). Immunofluorescence visualization of germ-line-specific cytoplasmic granules in embryos, larvae, and adults of *Caenorhabditis elegans*. *Proc. Natl. Acad. Sci. USA* **79**, 1558-1562.
Strome, S. and Wood, W. B. (1983). Generation of asymmetry and segregation of germ-line granules in early *C. elegans* embryos. *Cell* **35**, 15-25.
Sun, Y., Wilson, M. P. and Majerus, P. W. (2002). Inositol 1,3,4-trisphosphate 5/6-kinase associates with the COP9 signalosome by binding to CSN1. *J. Biol. Chem.* **277**, 45759-45764.
Uhle, S., Medalia, O., Waldron, R., Dumdey, R., Henklein, P., Bech-Otschir, D., Huang, X., Berse, M., Sperling, J., Schade, R. et al. (2003). Protein kinase CK2 and protein kinase D are associated with the COP9 signalosome. *EMBO J.* **22**, 1302-1312.
Ye, X., Nalepa, G., Welcker, M., Kessler, B. M., Spooner, E., Qin, J., Elledge, S. J., Clurman, B. E. and Harper, J. W. (2004). Recognition of phosphodegron motifs in human cyclin E by the SCF Fbw7 ubiquitin ligase. *J. Biol. Chem.* **279**, 50110-50119.